

photoconductivity at liquid nitrogen temperatures due to this absorption were unsuccessful. An appreciable photoconductive response was observed, however, in various *n*- and *p*-type specimens at liquid helium temperatures. Using a residual ray monochromator with five crystal quartz plates and a rock salt shutter, it was possible to demonstrate a response as far out as 23 microns.² Spectral response measurements were subsequently carried out with a Perkin-Elmer monochromator having interchangeable NaCl, KBr, and KRS-5 prisms.

The spectral response of a relatively pure *n*-type silicon specimen containing 4×10^{15} charge carriers/cm³ at room temperature is given in Fig. 1. The photoconductive response is proportional to

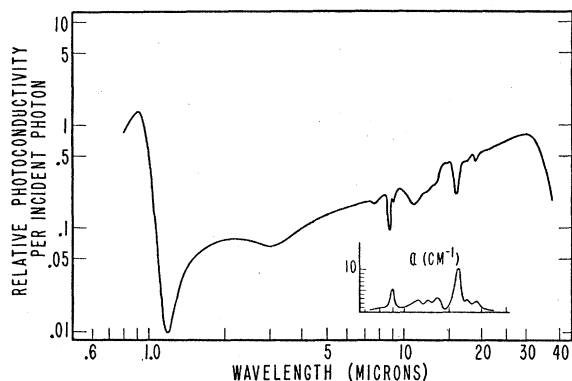


FIG. 1. The relative photoconductive response per incident photon of a relatively pure *n*-type silicon specimen containing 4×10^{15} charge carriers/cm³ at room temperature. The strong dip in the photoconductive response at 1.2 microns is due to the superposition of a photonegative response at the absorption edge. The dips in the photoconductive response appearing between 8 and 24 microns correspond to the peaks in optical absorption due to lattice vibrations which compete with the photoionization absorption by the neutral impurities. The room temperature absorption spectrum of silicon due to lattice vibrations is given in the insert.

the light intensity, extends to 38 microns (the limit of measurement), and is a maximum at 32 microns. The time constant of the photoconductive response as determined by square wave chopping was found to be less than 10^{-4} second. The room temperature absorption spectrum of silicon due to lattice vibrations³ is given in the insert in Fig. 1.

It is of interest to note that the dark resistance of the various *n*- and *p*-type silicon specimens at liquid helium temperatures was considerably smaller than the values expected from the ionization energies and concentrations of the impurities. By enclosing the specimen in a light-tight box with a shutter, it was found that the true dark resistivity of the relatively pure *n*-type silicon specimen at liquid helium temperature was greater than 10^{12} ohm-cm. With the shutter open to background radiation, the resistivity dropped to 5×10^7 ohm-cm. The fractional change in resistivity of other specimens with higher impurity concentrations were, however, less than 1 percent when the shutter was opened and closed. In general, the larger the impurity content, the lower the residual resistance at liquid helium temperature, and also the smaller the photoconductive response. It appears therefore that specimens with relatively high impurity concentrations contains an appreciable fraction of impurities which have very small ionization energies.

According to the theory for the simple hydrogen model the photoionization absorption cross section of the neutral impurities may be expected to increase with wavelength to a maximum value at the ionization limit. Under conditions where the density of impurities is sufficiently small, such that the product of absorption constant and the thickness of the photoconductor is very much less than unity, the photoconductive response will be proportional to the absorption cross section and will likewise attain a maximum value at the ionization limit. The optical ionization energy of the neutral impurities may thus be obtained from the position of the peak in the spectral response curve, provided there is no appreciable distribution of impurity levels. The data of Fig. 1 yields a

value of 0.04 eV for the optical ionization energy of the donor impurities in the relatively pure *n*-type specimen, which is somewhat smaller than the value 0.06 eV for the thermal ionization energy derived from Pearson and Bardeen's data for specimens of comparable impurity content.⁴

We wish to express our thanks to Dr. W. Shockley, Dr. J. Bardeen, and Mr. H. B. Briggs of the Bell Telephone Laboratories for helpful discussions and for supplying many of the specimens used in this investigation; to Dr. H. Stauss and Mr. J. Hino of the Metallurgy Division, Naval Research Laboratory, for making available specimens of pure silicon; and to Mrs. Bertha W. Hervis and Mr. H. Lipson of the Crystal Branch, Metallurgy Division, for their assistance in this investigation.

- ¹ Burstein, Oberly, Davisson, and Hervis, Phys. Rev. **82**, 764 (1951).
² Burstein, Oberly, and Davisson, Naval Research Laboratory Report of Progress, (July, 1950), p. 38 (unpublished).
³ E. Burstein and J. J. Oberly, Phys. Rev. **78**, 642 (1950).
⁴ G. L. Pearson and J. Bardeen, Phys. Rev. **75**, 865 (1949).

Asymmetric Fission

PETER FONG*

Department of Physics, University of Chicago, Chicago, Illinois

(Received October 2, 1952)

THE calculations by Frankel and Metropolis¹ have shown that at the saddle point of the energy in the fission process the nucleus is symmetric. However, at this point, there is practically no indication of a "neck," at which the deformed nucleus might break. The calculations by Hill² demonstrate that the fission process is slow enough that surface waves travel from one end to the other many times before a definite neck develops and fission occurs. In this letter it is proposed that the mode of fission is still undetermined at the saddle point. The concept of statistical equilibrium used by Bohr and Wheeler³ is extended from the saddle point to a much later stage when the fission fragments are just about ready to come apart. Accordingly the number of quantum states at that later stage will determine the relative probability of different modes of fission. For convenience of calculation the situation at the breaking point is represented by a simplified picture, namely, that of the two fragment nuclei of mass A_1 and A_2 in contact.

The fact that the number of quantum states for asymmetric fission is larger than that for symmetric fission is due mainly to the fact that the internal excitation energy of the fragments at the breaking point is larger for the asymmetric than for the symmetric mode. According to the model adopted, the excitation energy at the breaking point is

$$E = M^*(A, Z) - M(A_1, Z_1) - M(A_2, Z_2) - E_{e1} - D. \quad (1)$$

Here $M^*(A, Z)$ indicates the mass of the original excited fissioning nucleus, $M(A_1, Z_1)$ and $M(A_2, Z_2)$ the masses of the two fission fragments in their ground states, and E_{e1} the electrostatic repulsion between the two fragments. Since the nuclei are presumably highly deformed, a deformation energy D is introduced which decreases the energy available for distribution among the internal quantum states of the fragments. D is roughly independent of the mode of mass splitting and is estimated to be about 9 Mev. The term $-E_{e1}$, being proportional to $Z_1 Z_2$, favors asymmetric fission. The mass terms, according to the liquid drop model mass values calculated by Metropolis and Reitwiesner,⁴ favors symmetric fission. For example, the sum of masses of two equal fragments, Cd¹¹⁸, is lower than that of two fragments of the experimentally most probable mode, Zr¹⁰⁰ and Te¹³⁶, by 4.2 Mev. However, the liquid drop model mass values, compared to mass spectrometric ones, have shown errors of the order of 10 Mev. The masses of Cd¹¹⁸, Zr¹⁰⁰, and Te¹³⁶, though not yet determined experimentally, can be extrapolated from the masses of stable nuclei⁵ and from the parabolic dependence⁶ of mass on charge number. The results show that the mass of Cd¹¹⁸+Cd¹¹⁸ is higher than

Zr¹⁰⁰+Te¹³⁶ by 2 Mev, favoring asymmetric fission. This, together with the contribution from the $-E_{e1}$ term, causes E for asymmetric splitting to be larger than E for symmetric splitting by 4.5 Mev. Accordingly the asymmetric splitting will have a larger number of quantum states and so a larger probability of occurrence.

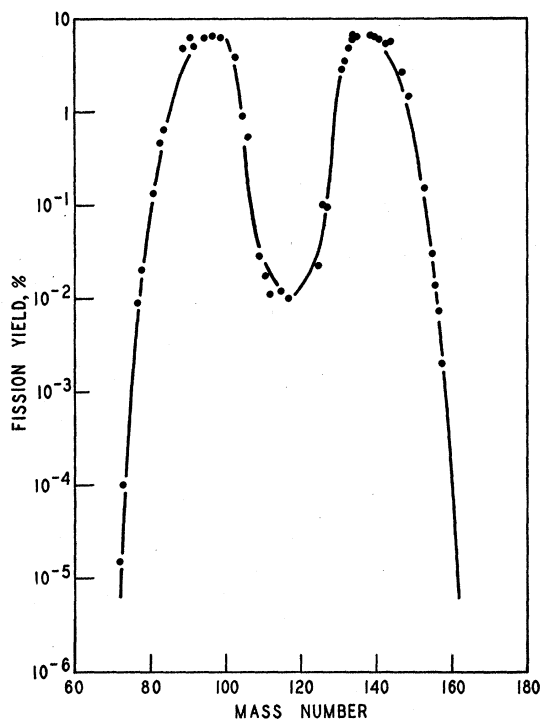


FIG. 1. Calculated mass distribution curve of slow neutron fission of U²³⁵, compared with the corresponding fission yields as determined by radiochemical methods (solid circles).

In order to establish the quantitative relation between excitation energy and the number of quantum states, the following formula is derived:

$$N \sim c_1 c_2 \left(\frac{A_1^{5/3} A_2^{5/3}}{A_1^{5/3} + A_2^{5/3}} \right)^{3/2} \left(\frac{A_1 A_2}{A_1 + A_2} \right)^{3/2} \frac{(a_1 a_2)^{3/2}}{(a_1 + a_2)^{5/2}} \times \left(1 - \frac{1}{2[(a_1 + a_2)E]^2} \right) E^{9/4} \exp\{2[(a_1 + a_2)E]^2\}, \quad (2)$$

where c_1 , a_1 ; c_2 , a_2 are the constants of the level density formula,

$$W(E) = c \exp[2(aE)^{1/2}], \quad (3)$$

for the two fragment nuclei A_1 and A_2 , respectively. According to the statistical assumption, N is proportional to the relative probability of occurrence of fission products (A_1, Z_1) and (A_2, Z_2).

For thermal neutron fission, the average value of E is about 11 Mev.⁷ The difference of 4.5 Mev between asymmetric and symmetric modes is large enough, by (2), to give a yield ratio of about 600. For high energy fission, by 100-Mev neutrons, say, the average value of E is much larger (>50 Mev) so that the difference of 4.5 Mev becomes insignificant. Symmetric and asymmetric modes will then have comparable probability, as is experimentally observed.

In order to derive the mass distribution curve, E values of all possible mass splitting are calculated as was indicated above for Zr¹⁰⁰ and Te¹³⁶. The constants of (3) are determined from fast neutron capture cross-section data with special attention to the even-odd and magic irregularities.⁸ The mass distribution curve obtained for slow neutron fission of U²³⁵ is given in Fig. 1.

This theory can readily be applied to problems of charge distribution, kinetic energy distribution, energy dependence, variation with fissioning nuclei, fission neutrons, fine structure, spontaneous fission, and ternary fission. A detailed paper is in preparation. The author wishes to express his deep gratitude to Professors Maria Mayer and Enrico Fermi for their guidance and valuable suggestions. He is also indebted to Drs. C. D. Coryell, H. E. Duckworth, J. S. Fraser, L. E. Glendenin, D. J. Hughes, R. B. Leachman, J. M. Miller, A. C. Pappas, E. P. Steinberg, E. W. Titterton, and A. Turkevich for discussions and/or communication of their unpublished work.

* Present address: 3800 East Colfax Avenue, Denver 6, Colorado.

¹ S. Frankel and N. Metropolis, Phys. Rev. **72**, 914 (1947).

² D. L. Hill, Phys. Rev. **79**, 197 (1950).

³ N. Bohr and J. A. Wheeler, Phys. Rev. **56**, 426 (1939); N. Bohr, Phys. Rev. **58**, 864 (1940).

⁴ N. Metropolis and G. Reitwiesner, *Table of Atomic Masses* (Argonne National Laboratory, Chicago, 1950).

⁵ H. E. Duckworth and co-workers, Phys. Rev. **78**, 479 (1950); **79**, 188 (1950); **79**, 402 (1950); **82**, 130 (1951); **82**, 131 (1951); **82**, 468 (1951); **83**, 229 (1951); **83**, 1114 (1951). Interpolation is made to cover all masses in the fission product region.

⁶ The mass term $B_A(Z-Z_A)^2$ is used. The Z_A 's are determined from beta-decay energies compiled by K. Way and co-workers in *Nuclear Data*, National Bureau of Standards Circular No. 499 (1950). The B_A 's are those of reference 4.

⁷ The sum of E and D is equal to the total energy available for the emission of prompt neutrons and prompt gamma-rays, which has been estimated to be about 20 Mev [D. C. Brunton, Phys. Rev. **76**, 1798 (1949)]. As D is about 9 Mev, we find E to be about 11 Mev.

⁸ The constants so determined are:

$$a = 0.050A \text{ (Mev)}^{-1} \text{ and } c = 0.38e^{-0.0051A} \text{ (Mev)}^{-1},$$

where A is the mass number of the nucleus. The energy E of (3) is to be counted from a characteristic level [H. Hurwitz and H. A. Bethe, Phys. Rev. **81**, 898 (1951)] which we take to be the level of odd-odd nuclei ground states smoothed out of magic irregularities. Fast neutron cross sections are given by Hughes, Spatz, and Goldstein, Phys. Rev. **75**, 1781 (1949); D. J. Hughes and D. Sherman, Phys. Rev. **78**, 632 (1950), and Hughes, Garth, and Eggler (unpublished).

Atomic Mass of P³¹

K. OGATA AND H. MATSUDA

Department of Physics, Faculty of Science, Osaka University, Osaka, Japan

(Received November 3, 1952)

WITH a modified Bainbridge-Jordan type mass spectrograph, the details of which were described in a previous report,¹ the mass differences of the doublets, P³¹H¹-S³², P³¹(H¹)₂-S³²H¹ and (O¹⁶)₂-P³¹H¹, were measured. P³¹-P³¹H¹-P³¹(H¹)₂-P³¹(H¹)₃ and S³²-S³²H¹-S³²(H¹)₂ were used as mass calibration groups, in which the masses of H¹, P³¹, and S³² were assumed to be 1.00814, 30.984, and 31.982, respectively. The results obtained are given in Table I, together with other recent data.² The errors

TABLE I. Mass differences of doublets.

Doublet	No. of doublets (plates)	Mass difference 10 ⁻⁴ amu	Previous ^a work
P ³¹ H ¹ -S ³²	34 (3)	95.00 ± 0.10	94.95 ± 0.10
P ³¹ (H ¹) ₂ -S ³² H ¹	16 (2)	94.91 ± 0.12	
Weighted mean		94.96 ± 0.07	95.04 ± 0.20
(O ¹⁶) ₂ -P ³¹ H ¹	11 (1)	82.45 ± 0.12	82.49 ± 0.30

^a See reference 2.

given in Table I are the probable errors, which are the square roots of the sums of squares of the statistical errors and of mass calibration errors (0.04 percent).

From the above doublets, P³¹H¹-S³² and (O¹⁶)₂-P³¹H¹, the mass difference of (O¹⁶)₂-S³² was calculated to be 177.41 ± 0.14, which is in good agreement with the previously reported value,¹ 177.21 ± 0.08.

By combining the (O¹⁶)₂-P³¹H¹ doublet mass difference with that of some previously reported doublets, the Q values of P³¹(β , α)Si²⁸ and of P³¹(d , α)Si²⁹ can be calculated. The Q values thus obtained are compared with those measured directly in nuclear reactions,³ in Table II. They are in good agreement with